Multi-Scale Hydrogen Bonding and Microphase Separation Synergistically Engineered PolyurethanePolyurea (PU-PUa) as High-Performance Binder

Hao Wu , Xiaobao Chen , Yi Chi * , Weimin Song , Jinyao Li , Zhiqiang Cheng

Posted Date: 3 June 2026

doi: 10.20944/preprints202606.0236.v1

Keywords: polyurethane-polyurea (PU-PUa); binder; microphase separation; hydrogen-bonding network; mechanical behavior

 doi:10.20944/preprints202606.0236.v1

Article

Multi-Scale Hydrogen Bonding and Microphase Separation Synergistically Engineered Polyurethane-Polyurea (PU-PUa) as High-Performance Binder

Hao Wu [1], Xiaobao Chen [1], Yi Chi [1,2]*, Weimin Song [1], Jinyao Li [1], Zhiqiang Cheng [3]

[1] School of Civil Engineering, Central South University, 22 South Shaoshan Rd., Changsha, Hunan 410075, China

[2] School of Road and Bridge Engineering, Hunan Communication Polytechnic, Changsha, Hunan 410132, China

[3] Shanghai Road and Bridge Group Co. LTD., Shanghai 200433, PR China

* Correspondence: author: 42054098@qq.com; Tel. +86 15084939659

Abstract

In response to the increasing frequency of extreme climate events and the growing demand for sustainable infrastructure, pavement materials are urgently required to offer enhanced resilience, structural stability, and environmental adaptability. This study presents the design and synthesis of a novel polyurethane-polyurea (PU-PUa) pavement binder, engineered through a synergistic approach involving nanoscale microphase separation and a hierarchical hydrogen-bonding network. Using a one-step synthesis approach involving aliphatic isocyanate, polyaspartic ester, polytetramethylene ether glycol, and 1,4-butanediol, the PU-PUa achieves nanoscale microphase separation between hard and soft segments. Fourier transform infrared (FTIR) spectroscopy validates the formation of characteristic PU-PUa moieties and a multi-scale hydrogen-bonding network, where interactions within and between hard and soft segments serve as the structural foundation for performance enhancement of the system. Comprehensive evaluations demonstrates that the PU-PUa binder features excellent properties and it is highly adjustable. Viscosity measurements reveal that increasing the soft segment content (SSC) or incorporating an appropriate amount of diluent significantly reduces system viscosity, thereby improving workability during mixing and paving. Contact angle tests indicate that the hydrophobicity of PU-PUa can be effectively tuned by adjusting the SSC, offering a crucial approach for optimizing moisture damage resistance. Curing behavior analyses show that curing kinetics are governed by both SSC and curing temperature; reducing the SSC or raising the curing temperature accelerates strength development and shortens the curing period. Furthermore, the PU-PUa binder exhibits desirable mechanical performances, characterized by superior surface hardness (>80) and high adhesion to aggregate (>2 MPa), ensuring durable bonding and resistance to wheel abrasion. With a balanced tensile performance, the elongation at break of the PU-PUa binder can be adjusted within the range from 90% to 157%, while the tensile strength varies between 6 MPa and 14 MPa at an intermediate temperature, reflecting outstanding resilience and cracking resistance. Overall, this study develops PU-PUa as a promising high-performance and durable pavement binder based on molecular-to-macroscopic strategy, providing an innovative solution for resilient and sustainable high-performance pavements.

Keywords: polyurethane-polyurea (PU-PUa); binder; microphase separation; hydrogen-bonding network; mechanical behavior

 doi:10.20944/preprints202606.0236.v1

1. Introduction

With the increasing frequency of extreme climate events and a global commitment to sustainable development, it is imperative to enhance the resilience, structural toughness, and environmental safety of pavement materials to facilitate high-quality and sustainable development of highway transportation. Consequently, the development of novel pavement materials that achieve an optimal balance of high strength, elasticity, superior durability, and excellent workability has become a central research priority in road engineering.

Against this background, polymer-based pavement binders have gradually gained traction as promising alternatives to conventional asphalt. Materials such as epoxy resins, polyurethanes, and acrylates are increasingly employed in pavement overlays, bridge deck pavements, rapid repair materials, and porous friction courses due to their tunable mechanical properties, high bonding strength, and improved durability [1–6]. Among these, polyurethane (PU) binders stand out for their unique advantages: they offer excellent flexibility even at low temperatures, desirable abrasion resistance, fast curing at ambient temperatures, exceptional aggregate adhesion, and the ability to tailor mechanical performance through molecular design [7–12]. As a result, PU binders have been widely investigated for applications including pavement cold recycling, ultra-thin wearing courses, and asphalt modification.

However, despite these benefits, conventional PU binders suffer from several critical limitations when applied in pavement engineering. A primary concern is their pronounced moisture sensitivity; the parasitic reaction between isocyanate groups and ambient moisture often triggers foaming and internal porosity, which significantly compromises the structural integrity and durability of the pavement. Moreover, standard PU formulations frequently struggle to balance high-temperature stiffness with low-temperature crack resistance, making them susceptible to premature failure under cyclic traffic loads and extreme temperature fluctuations. Furthermore, most PU systems, especially those based on aromatic isocyanates, are vulnerable to weathering degradation and thermo-oxidative aging, resulting in surface yellowing, chain scission, and loss of mechanical properties over time [13–18]. These deficiencies necessitate the development of advanced molecular engineering strategies to optimize the internal architecture of PU-based materials for more resilient pavement systems.

In this context, polyurethane-polyurea (PU-PUa) copolymers have emerged as a highly promising next-generation binder. By incorporating polyurea (PUa) structures through the reaction of isocyanates with amine-terminated compounds (e.g., polyaspartic esters), the resulting PU-PUa system introduces strong urea linkages (-NHCONH-), which form significantly more robust hydrogen bonds than conventional urethane linkages (-NHCOO-). This unique feature drives a well-defined microphase separation structure with nanoscale hard segment domains acting as physical crosslinks, while the continuous soft segment phase provides excellent elasticity. Compared to conventional PU, PU-PUa offers several distinct advantages: (1) superior resistance to moisture and hydrolysis due to the higher density of stable hydrogen bonds and lower content of free isocyanate groups; (2) enhanced weatherability and anti-aging performance, especially when using aliphatic isocyanates; (3) tunable curing kinetics and extended pot life via the steric hindrance effect of polyaspartic esters, allowing better on-site constructability; (4) improved workability with lower viscosity at higher soft segment content (SSC); and (5) a unique combination of high strength, exceptional toughness, and elastic recovery, which is essential for withstanding repeated traffic loads and thermal stresses. These attributes make PU-PUa an ideal candidate for demanding pavement applications, including rapid repair materials, high-elasticity noise-reducing surfaces, bridge deck pavements, and durable porous friction courses.

Despite these theoretical advantages, the application of PU-PUa in pavement engineering is still in its nascent stages, with limited understanding of the fundamental correlation between multi-scale hydrogen bonding, microphase morphology, and macroscopic engineering performance. Specifically, the relationships between the molecular architecture (particularly the SSC), the resulting microphase morphology (from hard-segment continuous to soft-segment continuous), and the macroscopic mechanical performance—especially fracture toughness—have not been systematically

 doi:10.20944/preprints202606.0236.v1

elucidated for PU-PUa systems. Most existing studies lack a gradient design that spans the percolation threshold, leaving the optimal composition for balanced strength, ductility, and fracture resistance undiscovered. Furthermore, the regulatory mechanisms by which SSC influences workability, curing kinetics, and the non-monotonic fracture behavior remain poorly understood. Most existing studies lack a gradient design that spans the percolation threshold, leaving the optimal composition for balanced strength, ductility, and fracture resistance undiscovered. Furthermore, the regulatory mechanisms by which SSC influences workability, curing kinetics, and the non-monotonic fracture behavior remain poorly understood.

Therefore, this study aims to develop a novel PU-PUa pavement binder through a rational molecular design and a streamlined one-step synthesis. By systematically investigating the interplay between segment composition, hydrogen-bonding interactions, and microphase separation, this research elucidates the reinforcing mechanisms governing the binder's rheological behavior, curing kinetics, and mechanical robustness. The findings provide a theoretical foundation and a practical framework for engineering high-performance, sustainable binders for next-generation resilient pavements.

2. Objective and Scope

This study aims to design a novel polyurethane-polyurea (PU-PUa) binder via a one-step synthesis process, leveraging multi-scale hydrogen bonding and nanoscale microphase separation. The primary objective is to establish the relationships between the molecular structures and properties by systematically varying the soft segment content (SSC) in the copolymer system. The scope covers microstructural verification, evaluation of workability and curing behavior, assessment of surface/interfacial properties (contact angle, bonding strength, and adhesion states), and mechanical characterization (hardness, tensile properties, modulus). By correlating microscopic features with macroscopic performance across the transition from a hard-segment-continuous to a soft-segment-continuous microstructure, this work provides a comprehensive design framework for engineering workable, durable, and high-performance PU-PUa binders.

3. Materials

The material design strategically of PU-PUa incorporates an aliphatic isocyanate (HDI trimer) as the crosslinking core of the hard segments to provide rigid support, a polyether diol (PTMEG) as the soft segment to impart flexibility, and polyaspartic ester as an amine-based chain extender that works synergistically with BDO to form a hard segment microstructure characterized by strong hydrogen bonding and high structural regularity. This design deliberately induces a well-defined microphase separation structure. The fundamental properties of raw materials are listed in Table 1.

3.1. Aliphatic Isocyanate

A trifunctional aliphatic isocyanate with a cyclic molecular architecture was employed as the hard-segment precursor. This configuration provides high crosslinking density and rigid nodes, which facilitate the ordered aggregation of hard segments and promote distinct microphase separation. Such structural features are essential for optimizing the binder's mechanical modulus, tensile strength, and thermal stability. The chemical structure of the isocyanate is illustrated in Figure 1.

 doi:10.20944/preprints202606.0236.v1

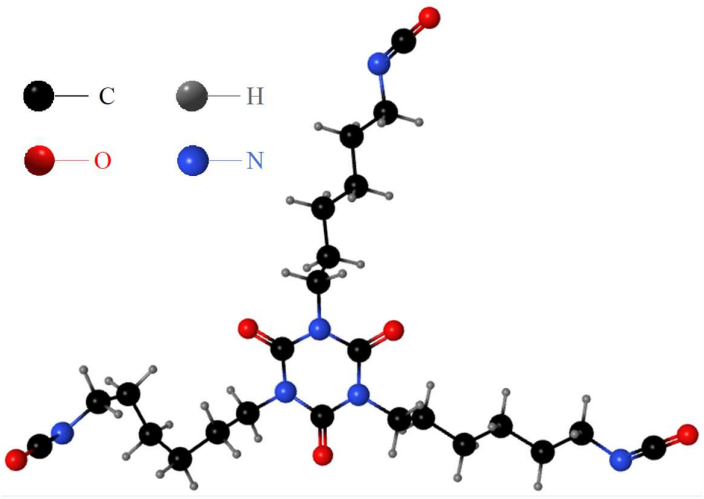

Figure 1. chemical structure of the isocyanate.

3.2. Polyether Diol

Polyether diol was selected to constitute the soft segments due to its intrinsic hydrolysis resistance and backbone flexibility, which are critical for pavement durability in humid and low-temperature environments. Compared to polyester-based diols, this polyether-type precursor offers superior hydrolytic stability and remains liquid at room temperature, ensuring better processing workability. Its chemical structure is presented in Figure 2.

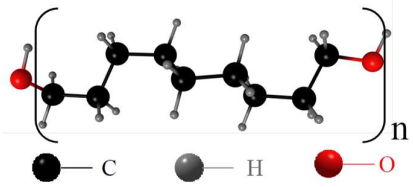

Figure 2. schematic diagram of polyether diol.

3.3. Polyaspartic Ester

The secondary chain extender used was a polyaspartic ester—a sterically hindered aliphatic secondary diamine synthesized from maleic acid and 3,3'-dimethyl-4,4'-diaminodicyclohexylmethane. The significant steric hindrance of this diamine regulates the reaction kinetics with isocyanates, effectively extending the pot life (working time) for field applications compared to primary amines. The chemical structure of polyaspartic ester is shown in Figure 3.

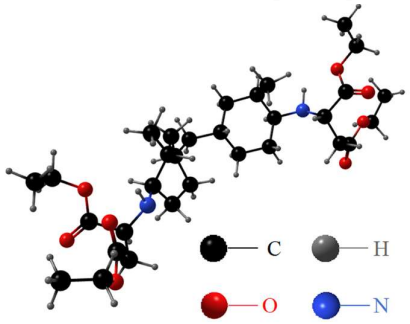

Figure 3. schematic diagram of polyaspartic ester.

The fundamental properties of the main materials for the synthesis of PU-PUa copolymer are summarized in Table 1.

 doi:10.20944/preprints202606.0236.v1

Table 1. Fundamental properties of raw materials.

Properties	Units	Test results		
		Isocyanate	Polyether diol	polyaspartic ester
Mass fraction of -NCO	%	21.70-22.20	N/A	N/A
Equivalent weight	g/mol	191	500	266
Viscosity (25℃)	mPa·s	1750	570	1250
Density	g/cm³	1.051	0.986	1.033
Color	APHA	≤ 40	≤ 50	≤ 230
Melting point	℃	-67	25	10
Flash point	℃	160	280	310

3.4. Additives

1,4-butanediol (BDO) was employed as a low-molecular-weight diol chain extender. Its lower reactivity compared to amine-based extenders allows for a more controlled polymerization process, while its linear structure facilitates the structural regularity of the hard-segment domains. To ensure the integrity of the cast specimens, a silicone-based defoaming agent (BYK 066N) was utilized to effectively eliminate micro-bubbles and prevent air entrapment during high-speed agitation, thereby minimizing internal defects and ensuring the reliability of mechanical characterizations. Additionally, ethyl acetate served as a diluent to optimize the system's rheological behavior and promote the homogeneous dispersion of resins and additives, ensuring the formation of a uniform crosslinked network. Moreover, if needed, resin-free color paste can also be added in the mixture for color adjustment.

3.5. Synthesis Mechanism of PU-PUa Copolymer

3.5.1. Synthesis of PU-PUa Copolymer

In this study, a one-step synthesis protocol was adopted to fabricate the PU-PUa copolymer, as illustrated in Figure 4. In the process, the isocyanate is first thoroughly mixed with polyether diol, after which all other raw materials are combined simultaneously and introduced into the reaction system.

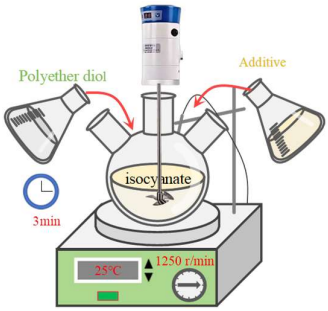

(a) one-step synthesis process

(b) PU-PUa copolymer

Figure 4. synthesis of PU-PUa copolymer.

Unlike the multi-stage prepolymer method, this approach involves the synchronous introduction of all reactive components, where the final elastomer architecture is governed by the differential nucleophilic reactivity of various hydrogen-containing functional groups toward the isocyanate. This “in situ” assembly facilitates the simultaneous evolution of a multi-scale hydrogen-bonding network and a nanoscale microphase-separated morphology. From an engineering perspective, this streamlined workflow significantly reduces processing complexity, energy consumption, and labor intensity, while the meticulous molecular design ensures that the resulting

 doi:10.20944/preprints202606.0236.v1

binder maintains superior structural integrity and mechanical performance tailored for pavement applications.

3.5.2. Copolymerization Mechanism of PU-PUa

The synthesis of PU-PUa involves a competitive polyaddition process. The synthesis of PU is typically performed through a polyaddition reaction between isocyanates (-NCO) and polyols. In contrast, PUa is synthesized via a polyaddition reaction involving isocyanates (-NCO) and polyamines[19,20].

PU: R-NCO+R′-OH→R-NH-COO-R′ (1)

PUa: R-NCO+R″-NH_2→R-NH-CO-NH-R″ (2)

When the precursor materials for PU and PUa (isocyanate, polyol, and amine compounds) are combined, the isocyanate group (-NCO) undergoes simultaneous reactions with both hydroxyl (-OH) and amine (-NH_2) groups, resulting in the formation of a PU-PUa copolymer. Therefore, the final product of the reactions is characterized by the presence of both urethane linkages (-NHCOO-) and urea linkages (-NHCONH-), forming a complex and cross-linked polymer network. The formation of PU-PUa copolymer can be represented as:

PU-PUa: $[\text{-NH-COO-R'-}]_x$ $[\text{-NH-CO-NH-R''-}]_y$ (3)

where, x and y denote the molar repetitions of the PU and PUa segments, respectively.

The core feature of the one-step process is the simultaneous or sequential occurrence of multiple competing reactions. Polyaspartic ester, a sterically hindered secondary amine, exhibits significantly higher reactivity than alcohols. During the initial mixing stage, the -NCO groups preferentially react with the -NH- groups of polyaspartic ester, generating hard segments containing highly polar urea bonds. This step is crucial for constructing a robust hydrogen bonding network and hard segment microstructure. Subsequently, BDO (a small-molecule primary alcohol) reacts with the isocyanate, further extending the hard segments. The primary hydroxyl groups of polyether diol also participate, connecting the flexible soft segment chains to the growing polymer network.

Due to the higher reaction priority of polyaspartic ester and BDO, hard segments composed of urea and urethane bonds are generated in situ. Driven by strong intermolecular forces (e.g., hydrogen bonding), these hard segments immediately aggregate upon formation. Unlike the prepolymer method—where the soft segment backbone is first synthesized and then hard segments are attached—the one-step process involves nearly simultaneous hard segment generation and microphase separation. As hard segment chains elongate, the system spontaneously undergoes nanoscale phase separation to reduce mixing enthalpy with the flexible polyether diol soft segments, forming hard segment microdomains dispersed within the soft segment matrix.

The steric hindrance of polyaspartic ester moderately retards urea bond formation, providing relaxation time for molecular chains to pack more orderly, thereby forming regular and effective hard segment microdomains. As a typical block copolymer, the PU-PUa molecular chains consist of alternating hard and soft segments connected by covalent bonds [21]. This chemical structure induces thermodynamic incompatibility between the segments, leading to a microphase separation structure—a key factor determining the mechanical properties of PU-PUa.

3.5.3. Molecular Composition of PU-PUa Copolymer

The molecular structure of the PU-PUa copolymer is rationally assembled from flexible long-chain polyether diols (soft segments), rigid isocyanate-derived moieties, and sterically hindered polyaspartic ester segments (hard segments). The molecular structure for the synthesis of PU-PUa and the resulting idealized PU-PUa structure are illustrated in Figure 5.

 doi:10.20944/preprints202606.0236.v1

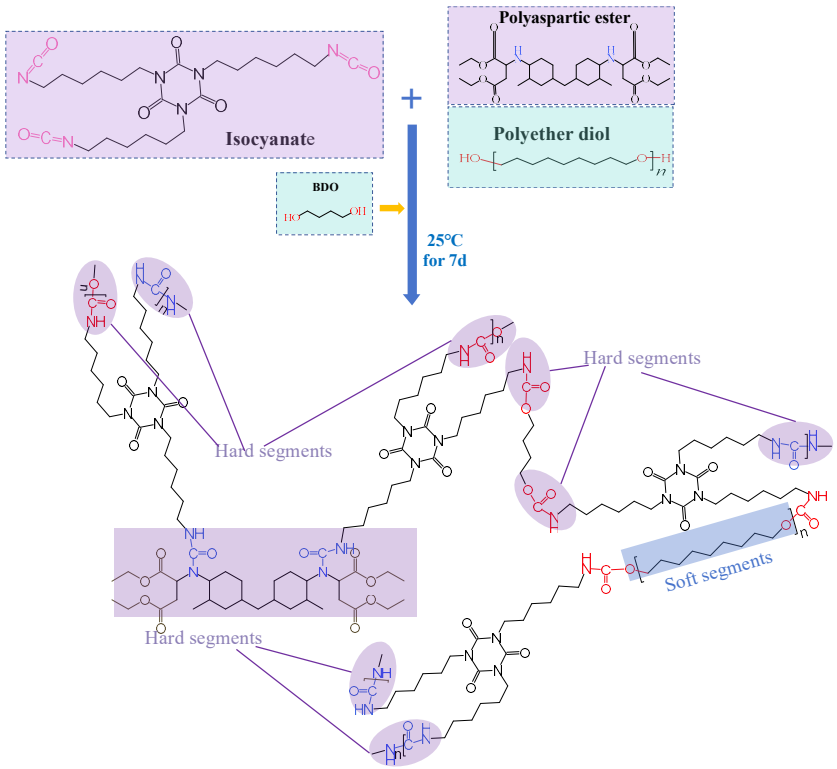

(a) molecular structures for synthesis of PU-PUa

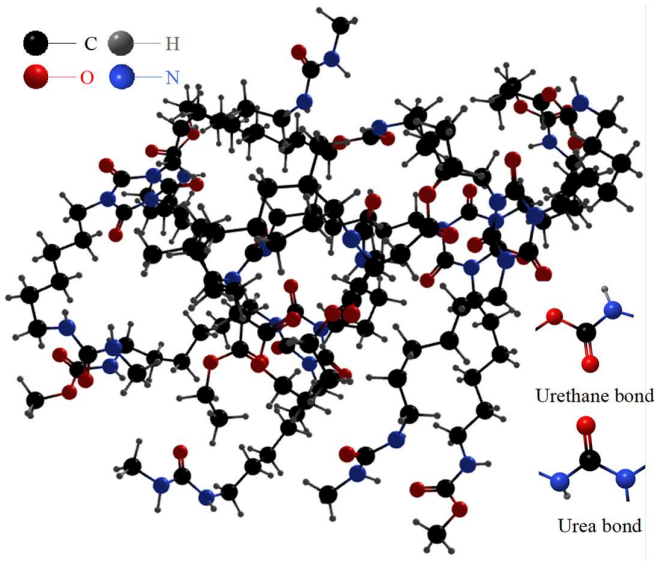

(b) idealized PU-PUa structure

Figure 5. molecular composition of PU-PUa copolymer.

The urethane linkage (-NHCOO-) serves as the fundamental repeating unit of the PU component. In this segmented block copolymer, the hard segments—formed by the polyaddition of diisocyanates and BDO—exhibit high polarity, which fosters an extensive network of inter-segmental hydrogen bonds. While the majority of these interactions occur within the hard domains to provide structural reinforcement, a secondary population of hydrogen bonds forms between the hard and

 doi:10.20944/preprints202606.0236.v1

soft segments. This hierarchical hydrogen-bonding network significantly enhances intermolecular cohesion, thereby dictating the material's macroscopic strength and elastic recovery.

Complementing the PU domains, the PUa segments are defined by the urea linkage (-NHCONH-). Compared to the asymmetric urethane group, the urea bond possesses a geometrically symmetric configuration and a higher density of hydrogen-bond donors (two NH groups per carbonyl). This bidentate hydrogen-bonding capability facilitates a significantly higher physical crosslinking density and thermodynamic stability. Therefore, the incorporation of PUa segments imparts superior environmental resilience to the binder, including enhanced resistance to thermo-oxidative aging, chemical ingress, and abrasive wear. Furthermore, the strong electron-donating effect of the nitrogen atoms in the urea group accelerates the reaction kinetics, enabling rapid, catalyst-free curing—a critical advantage for on-site pavement construction.

3.6. Mix proportions for PU-PUa copolymer

The PU-PUa developed in this study is intended for pavement materials, requiring both adequate mechanical performance and a sufficient workability. The formulation of PU-PUa was developed through a systematic empirical approach. First, exploratory tests and single-factor experiments identified viable dosage ranges for each component: isocyanate (30%–45%), polyaspartic ester (40%–55%), polyether diol (10%–28%), and BDO (0%–8%). Within these ranges, five representative formulations were selected to create a gradient of SSC (Table 2), enabling systematic investigation of the influence of SSC on macroscopic properties.

Table 2. Mix proportions for PU-PUa (mol).

Group	soft segment content (SSC)	Isocyanate	Polyaspartic ester	Polyether diol	BDO
PU-PUa-Ⅰ	14%	9.97	7.81	1.00	1.11
PU-PUa-Ⅱ	17%	7.85	4.80	1.00	1.54
PU-PUa-Ⅲ	20%	6.87	4.23	1.00	1.39
PU-PUa-Ⅳ	23%	5.89	3.84	1.00	1.01
PU-PUa-Ⅴ	26%	4.71	3.31	1.00	0.40

The design of these five formulations follows two key principles. First, the SSC is defined as the molar fraction of polyether diol relative to the total reactive components. SSC increases from 14% to 26% across Groups Ⅰ to Ⅴ, covering the typical transition from a hard-segment-dominated continuous phase to a soft-segment-continuous microstructure. This range intentionally spans the percolation threshold of hard segment microdomains, where the mechanical response shifts from rigid and high-strength to flexible and tough, allowing identification of an optimal balance for pavement applications.

Second, as the SSC increases, the molar ratios of isocyanate, polyaspartic ester, and BDO are simultaneously reduced. This coordinated decrease serves three purposes: (i) to maintain the overall stoichiometric balance between –NCO and reactive hydrogens (–OH from polyether diol and BDO, –NH from polyaspartic ester), ensuring complete reaction and minimizing residual isocyanate; (ii) to systematically dilute the density of urea and urethane linkages, thereby attenuating the physical crosslinking density of hard segment domains; and (iii) to avoid abrupt changes in the hard/soft segment interface, preserving a well-defined microphase separation structure across the composition range. In particular, the BDO content first increases from 1.11 (14% of SSC) to 1.54 (17% of SSC) and then gradually decreases to 0.40 (26% of SSC). This non-monotonic trend reflects an optimization of chain extension efficiency: at low of SSC, higher BDO helps extend hard segments and reinforce the rigid skeleton; at high SSC, excessive BDO would cause over-crosslinking and impair flexibility. Hence, the BDO variation is tuned to maintain the structural integrity of hard microdomains without sacrificing the compliance of the soft matrix.

 doi:10.20944/preprints202606.0236.v1

3.7. Chemical and Microstructural Characterization of PU-PUa Copolymer

Fourier transform infrared spectroscopy (FTIR) was employed to identify the characteristic absorption peaks and elucidate the microstructural characteristics of PU-PUa based on its chemical composition. The FTIR spectra are shown in Figure 6. The broad absorption peak at 3420 cm^{-1} is attributed to N-H stretching vibrations, and its broadened shape indicates extensive hydrogen bonding involving N-H groups. The peaks at 2930 cm^{-1} and 2850 cm^{-1} correspond to the asymmetric and symmetric stretching vibrations of CH_2, primarily originated from the methylene groups in polyether diol soft segments, confirming the presence of the soft segment phase.

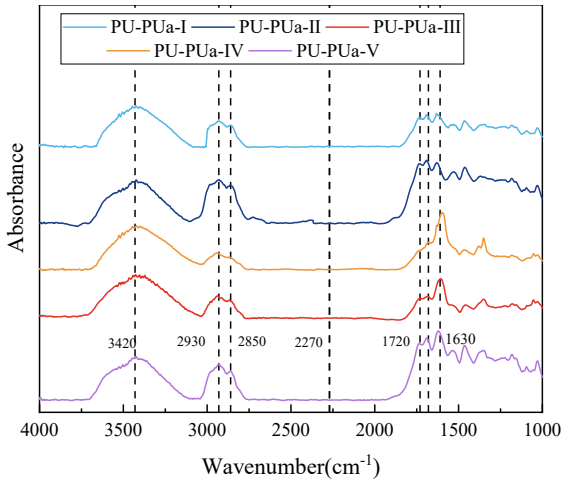

Figure 6. FTIR spectra of PU-PUa.

The characteristic absorption peak of isocyanate groups (-NCO) near 2270 cm^{-1} was not detected, indicating that the -NCO groups in the system were completely reacted, with no residual free -NCO. In the carbonyl (C=O) region, the distinct peak at 1720 cm^{-1} corresponds to the stretching of free urethane carbonyls within the PU domains. Whereas, the intense absorption at 1630 cm^{-1} is attributed to the stretching of urea carbonyls in the PUa segments. The relatively lower wavenumber of the urea peak compared to the urethane peak highlights the stronger hydrogen-bonding capability of the urea linkages, which underpins the superior structural stability of the PUa-rich hard domains.

Figure 7 presents a schematic diagram, clearly illustrating the molecular arrangement of soft and hard segments. Hard segments aggregate via intermolecular hydrogen bonding to form nanoscale physical crosslinking microdomains uniformly dispersed within the continuous soft segment matrix.

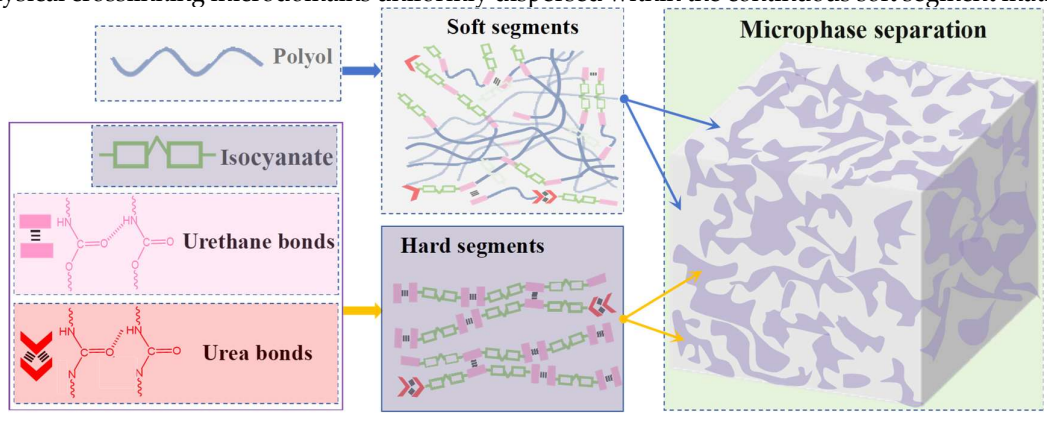

Figure 7. microphase separation structure of PU-PUa.

Atomic force microscopy (AFM) was used to understand the microphase separation structure of PU-PUa. Figure 8 showed AFM height images of the PU-PUa sample over a scan area of 0.5 μm × 0.5

 doi:10.20944/preprints202606.0236.v1

μm. The images provide visual confirmation of a well-defined "sea-island" morphology. The bright, elevated regions represent the high-modulus hard-segment phases (urethane and urea aggregates), while the darker, recessed regions correspond to the low-modulus soft-segment matrix. The observed topographical contrast stems from the difference in viscoelastic response between the two phases. These hard-segment "islands" function as effective physical crosslinking points, imparting high structural strength and deformation resistance. Simultaneously, the continuous soft-segment "sea" ensures excellent flexibility and elastic energy dissipation. This typical "sea-island" structure underpins the combination of high strength and high elasticity in PU-PUa: hard segment microdomains act as physical crosslinking points imparting strength and deformation resistance, while the continuous soft segment matrix governs flexibility and energy dissipation.

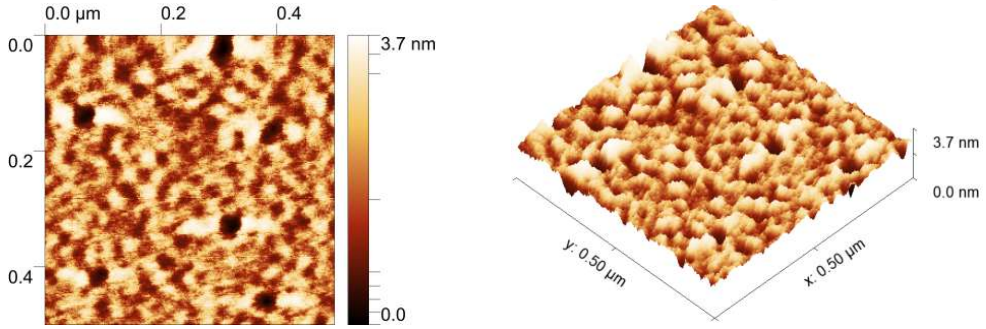

(a) 2D (b) 3D

Figure 8. morphology of PU-PUa.

4. Experimental Methods

4.1. Processing Characterization

The processing characteristics including viscosity and curing of the PU-PUa binder was systematically investigated by analyzing its transition from a liquid emulsion to a solid elastomer. This analysis allows for a comprehensive quantification of the binder's "working window" and its temperature-dependent strength development, which are critical for optimizing on-site construction protocols.

The dynamic viscosity of the PU-PUa binder was characterized using a rotational viscometer to assess its suitability for field applications. Measurements were conducted at 25°C utilizing a No. 27 spindle. The shear rate was varied within a range of 15 to 60 rpm to maintain torque readings between 10% and 98%, ensuring the linearity and accuracy of the rheological data. This evaluation provides critical insights into the binder's workability and its ability to sufficiently coat aggregate surfaces.

To further elucidate the influence of environmental conditions on the polymerization process, the viscosity evolution of the binder was monitored over time. Standard dumbbell-shaped specimens were initially cast and pre-cured at 25°C for 24 hours. Subsequently, isothermal curing was performed in constant-temperature chambers at 15°C, 25°C, 35°C, 45°C, and 60°C. Six replicates were prepared for each temperature group to quantify the relationship between thermal energy and the strength development rate of the PU-PUa system.

4.2. Interfacial Properties Between Binder and Aggregate

The hydrophobic and interfacial properties of PU-PUa binder and aggregate were evaluated through wettability, bonding strength, and boiling tests under dry and wet conditions. By correlating hydrophobic and interfacial properties with bonding performance, the compatibility of the system and its capacity to maintain long-term structural integrity in the presence of aggregate-binder interfaces were elucidated.

 doi:10.20944/preprints202606.0236.v1

4.2.1. Wettability test

The hydrophobic property of the PU-PUa were evaluated through static water contact angle (WCA) measurements, as shown in Figure 9. Deionized water droplets were deposited onto the specimen surface, and the contact angles were determined using a high-precision goniometer. To ensure statistical reliability, the average WCA was calculated from measurements taken at three distinct locations on each specimen.

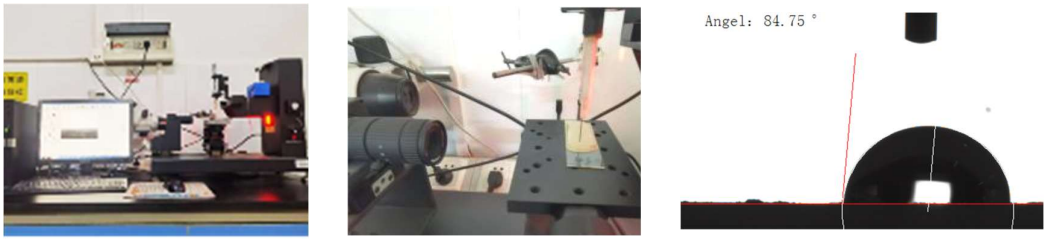

(a) contact angle meter (b) specimen during test (c) contact angle calculation

Figure 9. wettability test.

4.2.2. Interfacial Bonding Strength Test

The interfacial bonding strength between the binder and aggregate was evaluated using a pull-off test in accordance with ASTM D4541, as illustrated in Figure 10. The binder was uniformly applied onto the substrate surface, and then the pull-off dollies were placed onto the binder coating. A copper wire with a diameter of 0.2 mm was employed to control the thickness of the binder film between the dolly and the substrate, as shown in Figure 10(a). After the specimens had fully cured, the pull-off test was conducted, and the maximum pull-off force was recorded to calculate the bonding strength at the binder-substrate interface. Each test configuration was tested in triplicate to obtain the average interfacial bond strength.

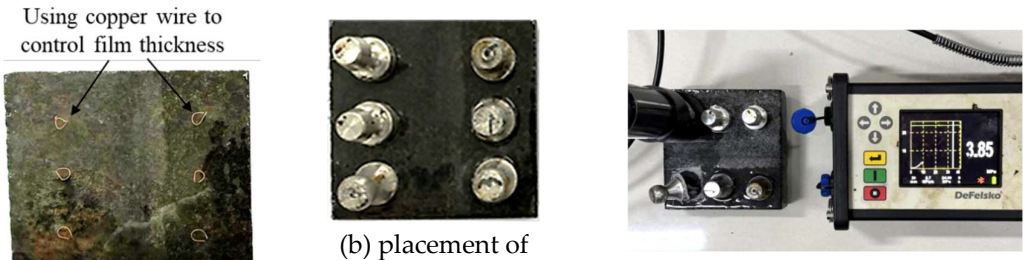

(a) substrate preparation (b) placement of pulling dollies (c) pull-off process

Figure 10. interfacial bonding test.

4.2.3. Boiling Test

The water stability of conventional polyurethane binders has always been a major concern when they are utilized as pavement binders, as their poor resistance to moisture attack can readily induce various distresses such as raveling and stripping in pavements. In this study, a modified boiling test based on ASTM D3625 was adopted to evaluate the adhesion state between the binder and aggregate under hydrothermal conditions, as illustrated in Figure 11.

 doi:10.20944/preprints202606.0236.v1

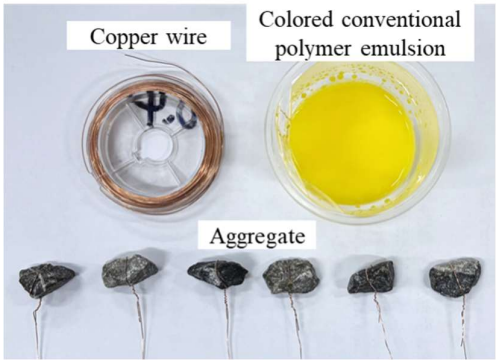

(a) specimen preparation

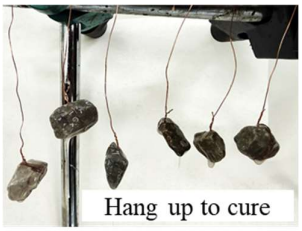

(b) curing of polymer coating

(c) prefabricate defect

(d) specimens under water erosion

Figure 11. modified boiling test.

First, aggregate particles with a size range of 9.5–13.2 mm were washed with deionized water to remove surface dust, then dried in an oven at 105 ± 5 °C to constant weight, and cooled to room temperature for subsequent use. Prior to coating, a copper wire was tightly wrapped around each aggregate particle. The aggregate was then completely immersed in the polymer or asphalt emulsion to ensure full coverage of its surface. The specimen was initially placed in gently boiling water for 3 min. Subsequently, the copper wire was withdrawn from the binder film on the specimen surface to create a prefabricated defect, thereby introducing a controlled circumferential weak interface within the cured binder film. This prefabricated defect allows peeling to initiate preferentially from this weakened region upon water exposure. Such a design enables a more reliable assessment of the intrinsic debonding resistance between the binder film and the aggregate surface.

After creating the defect, the specimens were further immersed in boiling water for another 10 min. Following the boiling treatment, the peeling behavior of the cured polymer or asphalt film from the aggregate surface was observed. Special attention was paid to whether peeling preferentially initiated at the prefabricated defects, thereby evaluating the interfacial stripping resistance between the polymer film and the aggregate.

4.3. Mechanical Performance Investigation

The mechanical integrity of the PU-PUa system was characterized through surface indentation and uniaxial tensile tests, as shown in Figure 12 and Figure 13. This combined evaluation of hardness and tensile behavior provides a holistic view of the binder's structural stability, specifically its ability to balance high-load bearing capacity with the elastic ductility required to accommodate traffic-induced strains.

 doi:10.20944/preprints202606.0236.v1

(a) sample

(b) indentation process

Figure 12. surface indentation test.

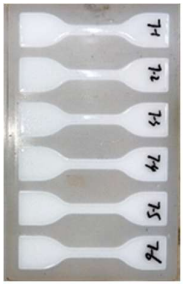

(a) sample

(b) tensile process

Figure 13. tensile test.

The surface resistance to indentation was measured using a Shore durometer. The specimens were placed on a rigid, level surface, and the hardness was recorded after the indenter maintained stable contact with the material. Three measurements were performed per sample to ensure consistency in the crosslinking density across the specimen surface. The mechanical strength and ductility of the PU-PUa binder were characterized through uniaxial tensile testing following ASTM D412. Dumbbell-shaped specimens were loaded to failure using a universal testing machine at a constant displacement rate of 50 mm/min. The tensile strength and elongation at break were recorded to evaluate the material's ability to withstand traffic-induced strain and resist fracture.

5. Results and discussion

5.1. Rheological Behavior and Workability

5.1.1. Influence of SSC on Viscosity

The rheological behavior of the PU-PUa system, specifically the influence of SSC on viscosity, is illustrated in Figure 14. The nascent viscosity of the binder is mainly governed by the intrinsic viscosity of the precursors and their instantaneous intermolecular associations. The initial viscosity for all formulations exceeded 500 mPa·s. This relatively high starting point is attributed to the cyclic structure of the isocyanate and the secondary amine structure of the polyaspartic ester, coupled with the intense hierarchical hydrogen bonding and dipole-dipole interactions between these highly polar species.

 doi:10.20944/preprints202606.0236.v1

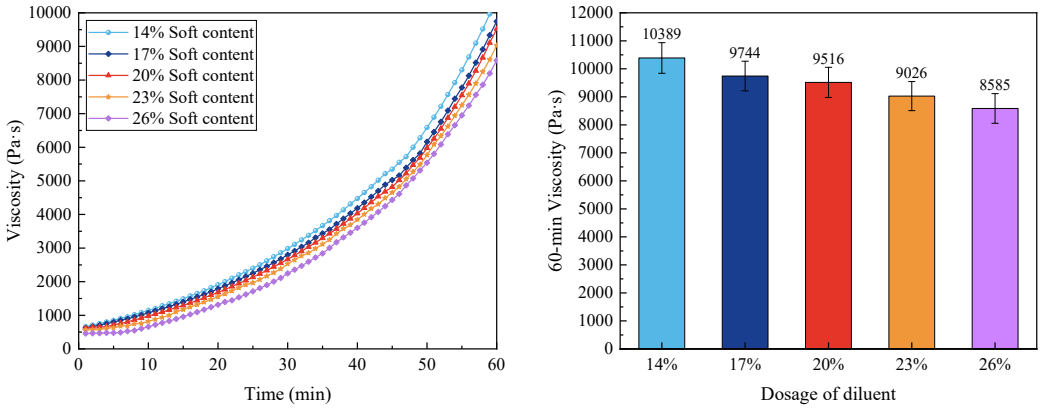

(a) Viscosity evolution with time (b) 60-minute viscosity

Figure 14. viscosity of PU-PUa with different SSC.

During the polymerization process, a progressive increase in viscosity was observed across all groups. At a constant diluent content of 4.5%, the 60-minute viscosity values with SSC of 14%, 17%, 20%, 23%, and 26% were recorded as 10,389, 9,744, 9,552, 9,026, and 8,585 mPa·s, respectively. This inverse relationship between SSC and viscosity indicates that the long-chain, flexible polyether diols function as an effective internal plasticizer. Increasing the SSC effectively lowers the relative concentration of the high-viscosity hard-segment precursors, thereby attenuating the density of urea-urea hydrogen bonds. Furthermore, although the ether oxygen atoms in the soft segments could engage in hydrogen bonding with the hard segments, these interactions are significantly weaker than the bidentate urea associations. Therefore, the proliferation of soft segments physically disrupts the formation of rigid physical crosslinking networks, leading to a more fluid rheological state.

5.1.2. Influence of Diluent on Viscosity

The impact of the external diluent on the rheology of PU-PUa system is further detailed in Figure 15. While the initial viscosities remained comparable across various diluent dosages, a dramatic divergence in the viscosity profiles emerged as the reaction progressed. At the 60-min mark, the viscosity with diluent dosages of 0%, 1.5%, 3.0%, and 4.5% were 51,670 mPa·s, 28,367 mPa·s, 16,930 mPa·s, and 9,026 mPa·s, respectively. Compared to the system without diluent, the viscosity of the systems with 1.5%, 3.0%, and 4.5% diluent were reduced by approximately 45.1%, 67.2%, and 82.5%, respectively. This demonstrated that the diluent was the most direct and effective means of regulating the viscosity, particularly by suppressing the rapid viscosity increased during the later stages, thereby significantly improving the workability of PU-PUa. This effect occurred because the diluent molecules intercalate between the growing polymer chains could increase the average intermolecular distance and provide a “screening effect” that effectively weakens the strong polar interactions. By systematically tailoring the SSC and diluent concentrations, the PU-PUa binder achieves an adjustable workability that accommodates the critical operational requirements of pavement construction, including mixing, hauling, and compaction process, thereby ensuring superior structural density and engineering quality.

 doi:10.20944/preprints202606.0236.v1

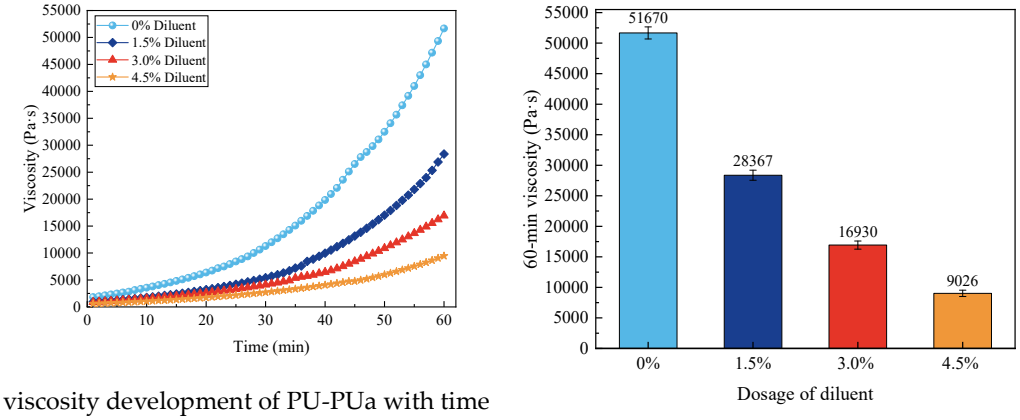

(a) viscosity development of PU-PUa with time

(b) 60-min viscosity

Figure 15. viscosity of PU-PUa with various diluent contents.

5.2. Curing Characteristic and Temperature Sensitivity

5.2.1. Influence of SSC on Curing Characteristic

The strength development profile of the PU-PUa system at 25°C as a function of SSC and curing time is presented in Figure 16. It can be seen clearly that the SSC is a decisive factor in the curing kinetics of the PU-PUa system. Formulations with lower SSC exhibited markedly accelerated early-stage strength gain. Specifically, after 24 hours of curing, the system with 14% SSC achieved 48.3% of its ultimate strength, whereas the system with 26% SSC reached only 28.1%, a nearly 1.7-fold difference in the growth rate. This disparity persisted through 72 hours, with 14% SSC, the system maintains a substantially higher degree of development (73.2%) compared to the 26% system (48.6%). This indicates that a lower SSC usually implies a higher relative concentration of high-reactivity isocyanate and polyaspartic ester precursors per unit volume. This increases the collision frequency of functional groups and accelerates the in-situ formation of a rigid urea/urethane-rich skeleton. Consequently, the system with 14% SSC reached the full strength at approximately 264 hours, while the 26% system required 336 hours at the same curing condition. These results suggest that tailoring the SSC is a highly effective strategy for enhancing early-age mechanical performance and compressing the curing process, which is essential for rapid-repair pavement applications.

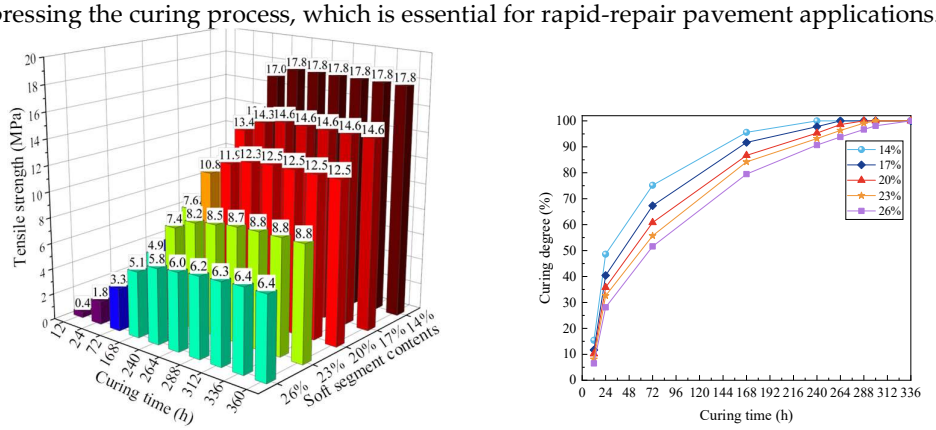

(a) Tensile strength

(b) Curing degree

Figure 16. strength development of PU-PUa with curing time.

 doi:10.20944/preprints202606.0236.v1

5.2.2. Influence of Temperature on Curing Characteristic

The synergistic influence of curing temperature and SSC on the overall curing cycle is further elucidated in Figure 17. It is distinct that increasing the curing temperature significantly reduced the curing time for all systems. However, the degree of this reduction varied considerably with different SSC. For the system with 20% SSC, elevating the curing temperature from 15 °C to 60 °C resulted in a dramatic 94% reduction in the total curing time (from 396 h to 24 h). This exponential acceleration is attributed to the enhanced thermal motion and increased effective collisions between reactive groups (-NCO and -NH/-OH), which concurrently promotes the ordering kinetics of the hard-segment microdomains within the microphase separation structure.

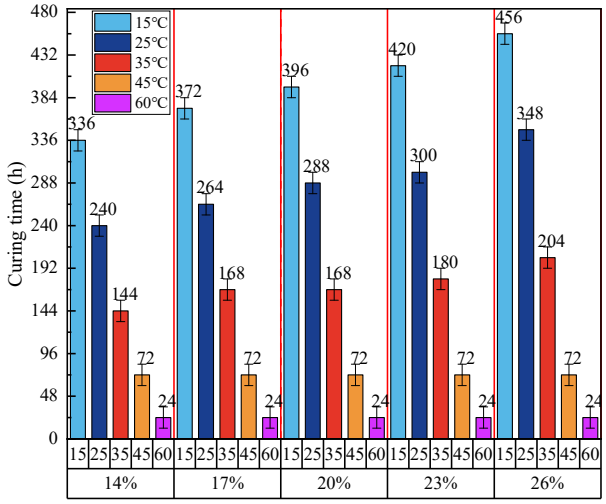

Figure 17. curing time of PU-PUa at various temperatures.

Furthermore, the sensitivity of the curing rate to SSC was temperature-dependent. In the low-to-moderate temperature range (15 °C–25 °C), the curing time for the system with 14% SSC decreased by 28.6% (from 336 h to 240 h), while the 26% system exhibited a 23.7% reduction. In this regime, the process is jointly governed by the chemical reaction rate and the diffusion-limited migration of molecular chains.

However, as the temperature increased further, this difference became more pronounced, in which a "kinetic convergence" was observed. In the high-temperature range from 45°C to 60°C, the curing time for the 14% system shortened from 72 hours to 24 hours, a reduction of 66.7%, while the curing time for the 26% system also decreased from 72 hours to 24 hours, exhibiting the same reduction rate. At these elevated thermal states, the reaction kinetics become dominated by the rapid polyaddition rate, which effectively masks the steric and mobility barriers associated with different soft-segment lengths.

Mastering these relationships between SSC, temperature, and strength evolution provides a scientific basis for optimizing mix designs and regulating curing protocols of the PU-PUa system. By dynamically adjusting construction plans according to environmental conditions, the curing duration can be significantly shortened, ensuring the rapid opening of resilient pavements to traffic.

5.3. Surface Wettability and Hydrophobicity

The surface characteristics of the PU-PUa binder, as quantified by static water contact angles, are presented in Figure 18. A clear inverse relationship was observed between the SSC and water contact angle. As the SSC increased from 14% to 26%, the water contact angle transitioned from a near-hydrophobic threshold of 90.0° down to 79.8°, 86.4°, 84.7°, 82.3°, and 79.8°, respectively. This trend indicates that higher SSC progressively enhances the surface wettability while compromising the intrinsic hydrophobicity of the material.

 doi:10.20944/preprints202606.0236.v1

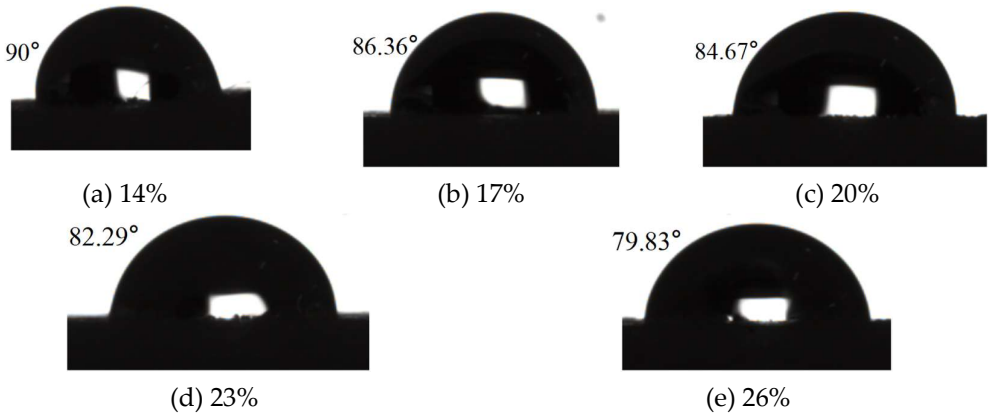

Figure 18. contact angles of different SSC PU-PUa.

The observed variation in water contact angle is fundamentally attributed to the thermodynamically driven surface reconstruction of the segmented copolymer. The hard segments (comprising isocyanate, polyaspartic ester, and BDO) are characterized by high cohesive energy density due to the dense network of urea and urethane linkages. From a thermodynamic perspective, these highly polar domains tend to migrate toward the bulk interior to minimize the interfacial energy at the water-air interface. Conversely, the polyether-based soft segments, characterized by lower polarity and higher chain mobility, preferentially migrate and accumulate at the polymer surface.

As the SSC increases in the polymer system, the surface enrichment of polyether chains becomes more pronounced. Although the alkane backbones in the soft segments are relatively non-polar, the increasing density of ether oxygen atoms, which can act as hydrogen-bond acceptors for water molecules elevates the surface free energy of the binder. Thereby, the surface of the polymer becomes more hydrophilic, leading to the observed reduction in contact angle.

In pavement engineering, the moisture susceptibility of the binder is a critical determinant of long-term structural durability. A higher contact angle (as seen in the formulations with a low SSC) facilitates the formation of a solid hydrophobic barrier on the aggregate surface. This barrier effectively repels moisture infiltration and suppresses capillary suction within the mixture's pore structure [22], and thus mitigating potential stripping and moisture-induced damage. Accordingly, optimizing the SSC to maintain a superior hydrophobic state is essential for ensuring the moisture stability of PU-PUa-based binder for pavement materials.

5.4. Interfacial Adhesion to Aggregate

5.4.1. Bonding Strength

The interfacial adhesion performance of the PU-PUa binder, as evaluated by pull-off tests on basalt substrates, is illustrated in Figure 19. A negative correlation was observed between the SSC and the pull-off strength. As the SSC increased from 14% to 26%, the pull-off strength systematically decreased from 3.95 MPa to 2.65 MPa. Even at the highest SSC (26%), the binder's adhesion strength (2.65 MPa) remained much higher than the typical value of conventional SBS-modified asphalt (1.75 MPa), underscoring the superior bonding capability of the PU-PUa system.

 doi:10.20944/preprints202606.0236.v1

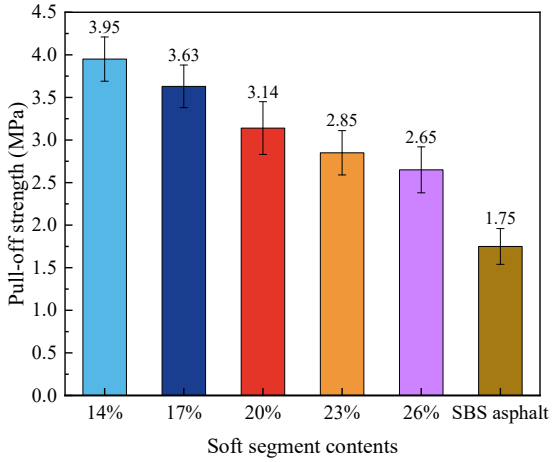

Figure 19. results from pull-off tests.

The observed degradation in pull-off resistance with increasing SSC is primarily rooted in the structural attenuation of the hierarchical hydrogen-bonding network. The urea bonds (-NHCONH-), formed through the precise reaction of isocyanates and amine-functionalized polyaspartic esters, constitute the high-polarity hard segments [23,24]. These segments drive the formation of rigid microdomains and provide the requisite cohesive strength through dense, bidentate hydrogen bonding. As the SSC increases, the spatial density of these urea-urea associations is effectively diluted, leading to a reduction in the physical crosslinking density of the hard-segment skeleton.

While secondary hydrogen bonds between hard and soft segments (e.g., N–H···O=C or N–H···O-ether) persist, their bond energies are significantly lower than those of the primary urea-urea interactions. As a results, the increasement of soft segments cannot thermodynamically compensate for the loss of cohesion caused by the fragmentation of the hard-segment domains. In pavement applications, this reduction in cohesive integrity manifests macroscopically as a decline in pull-off strength. However, the interfacial bond maintained by the remaining polar groups could still ensure an adhesion strength consistently exceeding 2.0 MPa. This exceptional bonding performance is a critical factor in enhancing the raveling resistance of the mixture and ensuring the long-term durability of the pavement under heavy traffic loads and environmental erosions.

5.4.2. Adhesion State of Polymer Binders to Aggregate After Water Erosion

Figure 20 illustrates the adhesion state of polymer binders to aggregate surfaces after water erosion. The PU-PUa binder exhibited exceptional adhesion to the aggregate. After immersion in boiling water at 100 °C for 10 min, no visible interfacial deterioration was observed between the PU-PUa film and the aggregate. The film surface remained smooth, and no obvious peeling or blistering occurred even at the prefabricated copper-wire defect (Figure 20(a)), indicating that the hierarchical hydrogen-bonding network and the intrinsic hydrophobicity of PU-PUa effectively suppress water infiltration along the interface.

 doi:10.20944/preprints202606.0236.v1

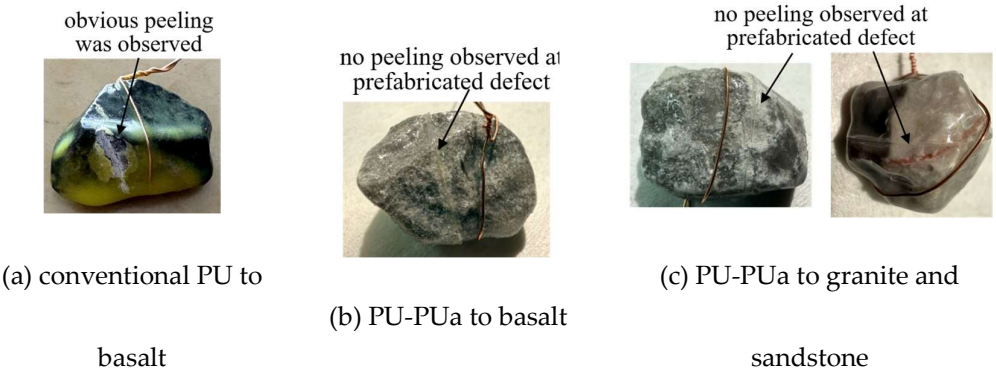

Figure 20. adhesion state of polymer binders to aggregate.

In contrast, the interface between conventional PU and the aggregate shown in Figure 20(c) changed noticeably after boiling-water exposure, with bubbles and peeling appearing at the prefabricated defect of the film, suggesting that the hydrothermal environment weakened its interfacial stability. Accordingly, compared with conventional PU, PU-PUa maintains a more stable interfacial structure and higher debonding resistance after boiling-water exposure, confirming its superior adhesion to aggregates. In addition, whether for acidic (granite and sandstone) or alkaline (basalt) aggregates, PU-PUa exhibits excellent aggregate adhesion, which is significantly superior to that of asphalt-based materials.

5.5. Mechanical Performances

5.5.1. Hardness

The Shore A hardness of the PU-PUa binder as a function of SSC is presented in Figure 21. The results reveal a pronounced sensitivity of surface hardness to the segmented composition. As the SSC increased from 14% to 26%, the hardness at 25 °C decreased from 97 to 81, representing a 16.5% reduction, while at 60 °C it decreased from 83 to 51, representing a 38.6% reduction in indentation resistance. This trend is intrinsically governed by the spatial density of the rigid physical crosslinking network. The hard segments, characterized by dense urea-urea hydrogen bonding, act as a framework that provides the material with its requisite stiffness and resistance to localized deformation. As the SSC increases, the volume fraction of these rigid domains is effectively diluted, leading to an attenuation of the physical crosslinking density. Furthermore, elevated temperature exacerbates this softening by enhancing molecular chain mobility and weakening hydrogen bond interactions, resulting in a more pronounced hardness drop at 60 °C.

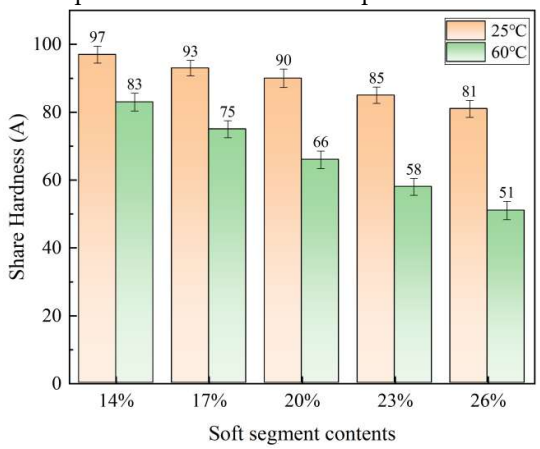

Figure 21. Hardness of PU-PUa.

 doi:10.20944/preprints202606.0236.v1

The evolution of hardness serves as a primary indicator of the material's abrasion resistance and long-term surface durability [25,26]. In pavement engineering, the dominant damage modes are fatigue wear induced by repeated traffic loading and abrasive wear caused by hard particles; under such conditions, a certain level of hardness is advantageous. However, excessively high hardness—associated with very low SSC—tends to induce brittle fracture and poor impact resistance, while excessively low hardness—arising from high SSC—may compromise structural support and accelerate wear. Therefore, the optimal wear performance likely resides in an intermediate range of SSC, where the hard-segment microdomains provide effective frictional energy dissipation barriers while the soft-segment matrix ensures elastic recovery and prevents catastrophic surface failure. From a microscopic perspective, the hard-segment microdomains serve as the primary barrier against frictional energy dissipation. As this barrier is weakened by higher SSC, the elastic recovery of the soft segment matrix may be insufficient to fully compensate for the loss of structural rigidity, potentially accelerating the wear process.

In pavement engineering, the selection of SSC should be strategically tailored to the specific service environment. For heavy-duty traffic sections requiring high-modulus characteristics, a lower SSC formulation (e.g., 14–17%) is recommended to ensure structural longevity. Conversely, for pavement structures subjected to significant thermal fluctuations or requiring enhanced strain accommodation, a moderately higher SSC can be utilized to optimize the balance between flexibility and surface protection.

5.5.2. Tensile Properties

The mechanical behavior of the PU-PUa binder were analyzed through tensile tests. The typical stress-strain curves and the evolution of mechanical performances (tensile strength and elongation at break) as a function of SSC are illustrated in Figure 22.

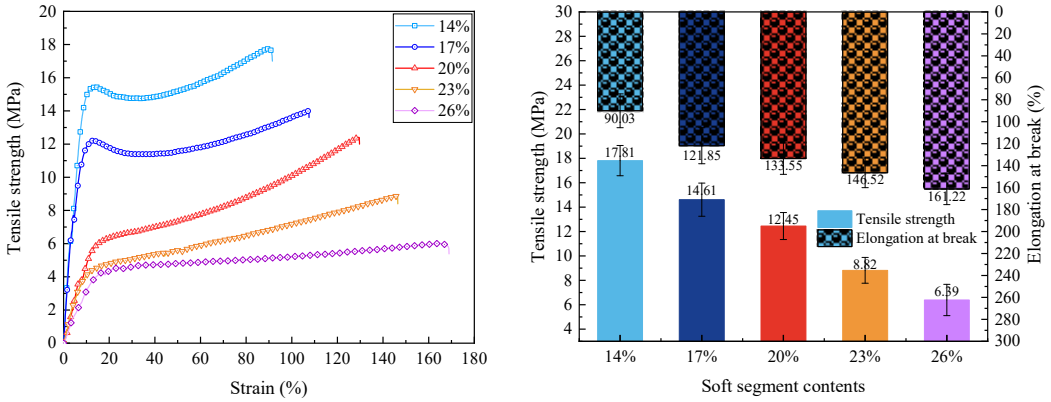

(a) Tensile strength vs. strain (b) Tensile strength and elongation at break

Figure 22. Tensile properties of PU-PUa.

The experimental results demonstrate a significant regulatory effect of the SSC on the mechanical response of the PU-PUa system. As shown in Figure 22(a), the stress-strain profiles undergo a distinct transition from a high-modulus, quasi-brittle behavior to a compliant, high-ductility response with increasing SSC. Quantitatively, as the SSC increased from 14% to 26%, the tensile strength markedly decreased from 17.81 MPa to 6.39 MPa (a 64.4% reduction), while the elongation at break systematically rose from 90.03% to 161.22% (a 78.9% increase).

Statistical analysis reveals a linear correlation within the investigated range: for every 1% increase in SSC, the tensile strength declines by approximately 0.96 MPa, whereas the elongation at break gains an average of 5.81 percentage points. This inverse relationship highlights the classic strength-ductility balance inherent in segmented copolymers, where the material can be precisely

 doi:10.20944/preprints202606.0236.v1

tailored to meet specific pavement requirements, ranging from high-strength structural reinforcement to high-toughness deformation accommodation.

This regular variation arose from the reconstruction of the microstructure. As the SSC increased, the proportion of hard segments composed of isocyanates and amine-based chain extenders correspondingly decreased, resulting in a reduced density of hard segment microstructure that formed the physical crosslinking network. Specifically, the dilution of the strong hydrogen bond network between urea bonds within the hard segment micro-structure directly weakened the load-bearing capacity. Meanwhile, the continuous soft segment phase provided greater freedom for molecular chain movement, enabling the material to undergo more significant plastic deformation after yielding and thereby exhibiting higher elongation at break. By precisely regulating the SSC, the material could be tailored from high strength with low elongation to low strength with high toughness.

When PU-PUa was used as a pavement material to replace asphalt or other polymer binders, it must withstand millions of repetitive loads during service. The exceptional fatigue performance stemmed from the synergistic effect of strength and toughness [27,28], which could enable the material to efficiently dissipate energy and delay micro-crack initiation and propagation under cyclic loading, potentially endowing the pavement with outstanding crack resistance and fatigue durability. Direct confirmation of this potential, however, required dedicated fatigue testing under cyclic loading conditions, which was a critical focus for the subsequent research.

5.5.3. Resilient Modulus

The resilient modulus of PU-PUa with varying SSC were presented in Figure 23. As the SSC increased from 14% to 26%, the elastic modulus monotonically decreased from 176.64 MPa to 24.39 MPa, representing a reduction of 86.2%, with the most pronounced decline (approximately 48.4%) occurring in the range of 17%–20%. This trend was attributed to the structural transition from a hard-segment continuous phase to dispersed microdomains. At low SSC, the hard segments formed a percolating rigid skeleton through a dense hydrogen bonding network, endowing the material with a high modulus. With increasing SSC, the physical crosslinking density of the hard segments decreased, and the soft segment continuous phase gradually dominated the elastic response, leading to a sharp reduction in modulus.

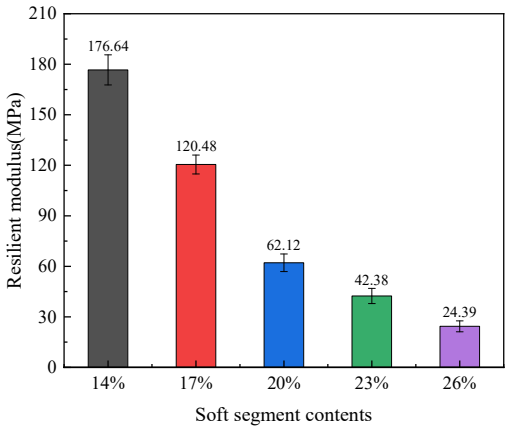

Figure 23. Resilient modulus of PU-PUa.

The resilient modulus directly influenced the material's rutting resistance and stress buffering capacity. High soft segment materials with low modulus were suitable for stress-absorbing layers or low-temperature crack-resistant scenarios, whereas low soft segment materials with high modulus were more appropriate for heavy-duty rigid pavements.

 doi:10.20944/preprints202606.0236.v1

5.5.4. Microstructural Mechanism Analysis

The observed evolution of mechanical properties is intrinsically governed by the reconstruction of the microphase-separated morphology. The hard segments, which form nanoscale physical crosslinking nodes via bidentate urea–urea hydrogen bonds, dictate the initial modulus and ultimate tensile strength of the system. As the SSC increase, the volumetric fraction of these rigid domains is progressively diluted, leading to a marked reduction in the density of the physical network. In particular, the attenuation of urea–urea associations—the strongest hydrogen bonds within the system—lowers the energy barrier for interchain slippage, thereby accounting for the observed decline in tensile strength.

Conversely, the systematic increase in elongation at break with rising SSC originates from two synergistic mechanisms: entropic elasticity and sacrificial bond dissipation. The continuous soft segment phase, comprising flexible polyether chains, offers enhanced conformational freedom, enabling substantial chain rearrangement and disentanglement after yielding. More importantly, the multi-scale hydrogen-bonding network (encompassing urethane–urea, urea–ether, and residual urethane–urethane interactions) functions as a hierarchy of reversible sacrificial bonds. Under high tensile strain, these weaker non-covalent linkages preferentially rupture prior to covalent bond scission, dissipating mechanical energy and shielding the polymer backbone from premature failure. This progressive, energy-dissipative mechanism effectively delays micro-crack initiation and propagation, endowing the PU-PUa system with a unique combination of strength and ductility that is highly desirable for pavement applications.

5.7. Comparison with conventional PU and asphalt binder

To benchmark the developed PU-PUa binder against existing pavement materials, its key properties were compared with conventional PU binders and typical SBS-modified asphalt, as summarized in Table 3. The data for PU and SBS-modified asphalt binders are compiled from typical values in representative studies. The PU-PUa data originate from the present study (SSC ranging from 14% to 26%).

Table 3. Comparison of PU-PUa, conventional PU, and SBS-modified asphalt.

Property	PU-PUa	Conventional PU [2,7,15,23,24]	SBS-modified asphalt [2,22,28]
Curing time (h, @25°C)	240 – 336	168 – 360	N/A (Thermoplastic)
Viscosity (mPa·s)	500 – 1000 (@25°C)	500 – 2000 (@25°C)	2000 – 5000 (@135°C)
Water contact angle (°)	80 – 90	70 – 85	80 – 95 (varies with aging)
Bonding strength (MPa)	2.6 – 4.0	1.2 – 3.0	0.6 – 1.5
Adhesion post-erosion	Intact	Severe peeling	Intact (Acid-sensitive)
Shore A hardness	81 – 97	70 – 90	N/A (very soft)
Tensile strength (MPa)	6.0 – 18.0	4.0 – 10.0	1.0 – 2.5
Elongation at break (%)	90 – 160	70 – 260	150–300 (@ 25°C), <50 (@ 5°C)

 doi:10.20944/preprints202606.0236.v1

PU-PUa achieves tunable tensile strength (6–18 MPa) and elongation (90–160% at 25 °C) with the variation of SSC, far exceeding SBS-modified asphalt (1–2.5 MPa). Its pull-off strength (2.6–4.0 MPa) is also significantly higher than that of asphalt (0.6–1.5 MPa) and ranks among the best PU binders. By adjusting SSC (14–26%), both strength and ductility can be tailored—a unique design flexibility. Moreover, its water contact angle (80–90°) can be increased by reducing SSC to enhance hydrophobicity and moisture resistance. In addition, PU-PUa is a cold-mix, cold-cure system with low initial viscosity (500–1000 mPa·s at 25 °C), enabling easy mixing and compaction at ambient temperature. Curing time (240–336 h at 25 °C) can be shortened to 24 h at 60 °C, ideal for rapid repair. Thanks to its hierarchical hydrogen-bonding network and nanoscale microphase separation, PU-PUa offers superior aging and hydrolysis resistance compared to conventional PU, while asphalt suffers from UV/thermal degradation.

Overall, PU-PUa bridges high-strength thermosets and flexible elastomers, surpassing conventional asphalt in adhesion, strength, and moisture resistance while offering broader tunability than typical PU binders. These advantages, rooted in the synergistic design of multi-scale hydrogen bonding and microphase separation, position PU-PUa as a next-generation binder for resilient and sustainable pavements.

6. Conclusion

This study synthesized PU-PUa copolymers with a distinct microphase separation structure and a multi-scale hydrogen bonding network using a one-step method. The intrinsic relationships among molecular structure, curing behavior, and macroscopic properties were systematically elucidated, providing a theoretical and experimental foundation for developing high-performance pavement binders. The main conclusions are as follows:

(1) Based on the molecular synergistic effect between aliphatic isocyanate and polyaspartic ester, a multi-scale hydrogen bonding network dominated by urea-based hydrogen bonds was constructed within the PU-PUa system, inducing the formation of a nanoscale microphase separation structure. In the PU-PUa system. Hard segment microdomains serves as physical crosslinking points imparting high strength, while the entropic elasticity recovery of soft segments and the reversible breaking/reformation of hydrogen bonds enable efficient energy dissipation and enhanced toughness.

(2) The workability and curing behavior of the PU-PUa system can be precisely controlled by adjusting the SSC and curing temperature. Increasing the SSC or adding a small amount of diluent significantly reduces viscosity, whereas decreasing the SSC or raising the temperature accelerates strength development and shortens the curing cycle. This adaptability provides a broad operational window for critical processes such as mixing, hauling, paving, and compaction, ensuring both construction quality and project efficiency.

(3) The surface wettability and interfacial adhesion of the PU-PUa binder are critically governed by the surface reconstruction of soft segment. Lowering the SSC enhances the intrinsic hydrophobicity, creating an effective moisture barrier on aggregate surfaces. Furthermore, the material maintains exceptional interfacial bonding states and Shore hardness, ensuring superior stripping resistance and long-term abrasion durability under the combined effects of moisture and repetitive traffic loading.

(4) The PU-PUa binder exhibits an outstanding strength-ductility combination, with tensile strengths ranging from 6.0 MPa and 18.0 MPa and elongations at break from 90% to 160 %. The rigid hard segment skeleton ensures high load-bearing capacity, while the synergistic toughening effect, enabled by the sacrificial bond mechanism, effectively retards micro-crack initiation and propagation. These properties endow the PU-PUa system with superior crack resistance and the potential for exceptional fatigue durability in resilient pavement applications.

 doi:10.20944/preprints202606.0236.v1

Conflicts of Interest: The authors claim no conflict of interest.

Acknowledgements: The authors are grateful for the finical supports from the Project of Hunan Provincial Department of Water Resources (No. XSKJ2025056-29) and the National Natural Science Foundation of China (No. 52478291).

References

1. Y. Chen, J. Hu, X. Wu, et al. Synthesis and Evaluation of Polyurethane as Waterproof Adhesion Layer for Steel Bridge Deck. Polymers, 2024, 16: 3140.
2. H. Wu, M. Yang, W. Song. Mechanical and Rheological Properties of Polyurethane-Polyurea (PU-PUa) Modified Asphalt Binder. Construction and Building Materials, 2024, 411: 134798.
3. L. Li, T. Yu. Curing Comparison and Performance Investigation of Polyurethane Concrete with Retarders. Construction and Building Materials, 2022, 326:126883.
4. W. Song, D. Chen, H. Wu. et al. Preparation and Performance Characterization of Waterborne Epoxy Resin Modified Asphalt Emulsion for Tack Coat. Journal of Cleaner Production, 2024, 475: 143715.
5. J. Lei, F. Fan, S. Xu, et al. Study on Mechanical Properties of Modified Polyurethane Concrete at Different Temperatures. Applied sciences, 2022, 12(6): 3184.
6. H. Wu, Z. Wu, W. Song, et al. Investigation on One-Component Waterborne Epoxy Emulsified Asphalt (OWEEA) Used as Bonding Material. Buildings, 2024, 14(2): 503.
7. M. Sobczak, C. Dębek, E. Olędzka, G. Nałęcz-Jawecki, et al. Segmented Polyurethane Elastomers Derived from Aliphatic Polycarbonate and Poly(ester-carbonate) Soft Segments for Biomedical Applications. Journal of Polymer Science, Part A: Polymer Chemistry, 2012, 50(18): 3904-3913.
8. N. Roohpour, J. Wasoloewocz, A. Moshaverinia, et al. Polyurethane Membranes Modified with Isopropyl Myristate as a Potential Candidate for Encapsulating Electronic Implants: A Study of Biocompatibility and Water Permeability. Polymers, 2010, 2(3):102-119.
9. H. Janik, M. Marzec, A Review: Fabrication of Porous Polyurethane Scaffolds. Materials Science and Engineering: C, 2015,12(2):586-591.
10. Y. Feng, W. Xia, J. Huang, et al. Thermo-Optic Response and Mechanical Properties of Hybrid Polyurethane Elastomers via Silicon Group-induced Microphase Separation Evolution. Reactive and Functional Polymers, 2023, 193: 105739.
11. L. Wang, S. Xiang, G. Ling, et al. New Modification Strategy for Thermoplastic Polyurethane with High Hygrothermal Ageing Resistance and Flame Retardancy. Polymer Degradation and Stability, 2025, 232: 111140.
12. D. Fu, W. Pu, Z. Wang, et al. A Facile Dynamic Crosslinked Healable Poly(oxime-urethane) Elastomer with High Elastic Recovery and Recyclability. Journal of Material Chemistry A, 2018, 6(37): 18154-18164.
13. X. Wang, H. Zhang, B. Yang, et al. A Colorless, Transparent and Self-healing Polyurethane Elastomer Modulated by Dynamic Disulfide and Hydrogen Bonds[J]. New Journal of Chemistry, 2020, 44(15): 5746-5754.
14. J. Chen, X. Ma, H. Wang, et al., Experimental Study on Anti-icing and Deicing Performance of Polyurethane Concrete as Road Surface Layer. Construction and Building Materials, 2018, 161: 598–605.
15. H. Wu, X. Chen, W. Song, et al. A Novel Polyurethane-Polyurea (PU-PUa) Binder for Porous Ultra-Thin Friction Course: Design, Characterization, and Performance Evaluation. Construction and Building Materials, 2025, 483: 141775.
16. S. Vlad, I. Spiridon, C. Grigoras, et al. Thermal, Mechanical and Wettability Properties of Some Branched Polyetherurethane Elastomers. Polymers, 2009, 9 (1): 37–47.
17. Y. Wang, L. Wang, H. Liu, et al. Polyurethane as Smart Biocoatings: Effects of Hard Segments on Phase Structures and Properties. Progress in Organic Coatings, 2021, 150: 106000.
18. Y. Guo, R. Zhang, Q. Xiao, et al. Asynchronous Fracture of Hierarchical Microstructures in Hard Domain of Thermoplastic Polyurethane Elastomer: Effect of Chain Extender. Polymer, 2018, 138: 242-254.
19. J. Rong, J. Zhong, W. Yan, et al. Study on Waterborne Self-Healing Polyurethane with Dual Dynamic Units of Quadruple Hydrogen Bonding and Disulfide Bonds. Polymer, 2021, 221: 1236525.

 doi:10.20944/preprints202606.0236.v1

20. Y. He, D. Xie, X. Zhang, The Structure, Microphase-Separated Morphology, and Property of Polyurethanes and Polyureas. Journal of Materials Science, 2014, 49(21): 7339-7352.
21. P. KROL, Synthesis Methods, Chemical Structures and Phase Structures of Linear Polyurethanes. Properties and Applications of Linear Polyurethanes in Polyurethane Elastomers, Copolymers and Ionomers. Progress in Materials Science. 2007, 52(6): 915–1015.
22. J. Paraguya, R. Dingcong, H. Bacosa. A Novel Inherently Hydrophobic and Physicomechanically Robust Coconut Oil-Based Polyurethane-Modified Mortar. Scientific Reports, 2025, 15: 40664.
23. S. Wu, S. Ma, Q. Zhang. A Review of polyurethane: Properties, Applications and Future Perspectives. Polymer, 2025, 327: 12361.
A. Gomez-Lopez, S. Panchireddy, B. Grignard. Poly(hydroxyurethane) Adhesives and Coatings: State-of-the-Art and Future Directions. ACS Sustainable Chemistry & Engineering, 2021, 9(29): 9541-9562.
24. K. Kwiatkowski, M. Nachman. The Abrasive Wear Resistance of the Segmented Linear Polyurethane Elastomers Based on a Variety of Polyols as Soft Segments. Polymers, 2017, 9(12): 705.
25. R. Beck, R. Truss. Effect of Chemical Structure on the Wear Behaviour of Polyurethane-Urea Elastomers. Wear, 1998, 218(2): 145-152.
26. N. Tran, R. Moraes, A. Taylor, et al. Field Performance of Asphalt Mixture Modified with Reactive Isocyanate-based Modifier. Canadian Journal of Civil Engineering. 2025, 52(3): 363-368.
27. H. Xu, L. Kong, Y. Zhang. Preparation and Characterization of Polyurethane Composite Modified Epoxy Resin for Novel Colored Anti-Skid Pavement Materials. Materials Letters, 2024, 369: 136760.